


3-2011

A Novel Pulsed Corona Discharge Reactor Based on Surface Streamers for NO Conversion from N₂-O₂ Mixture Gases

M. A. Malik
Old Dominion University

Karl H. Schoenbach
Old Dominion University

Follow this and additional works at: https://digitalcommons.odu.edu/bioelectrics_pubs

 Part of the [Biomedical Engineering and Bioengineering Commons](#), and the [Environmental Sciences Commons](#)

Repository Citation

Malik, M. A. and Schoenbach, Karl H., "A Novel Pulsed Corona Discharge Reactor Based on Surface Streamers for NO Conversion from N₂-O₂ Mixture Gases" (2011). *Bioelectrics Publications*. 36.
https://digitalcommons.odu.edu/bioelectrics_pubs/36

Original Publication Citation

Malik, M.A., & Schoenbach, K.H. (2011). A novel pulsed corona discharge reactor based on surface streamers for NO conversion from N₂-O₂ mixture gases. *International Journal of Plasma Environmental Science & Technology*, 5(1), 50-57.

A Novel Pulsed Corona Discharge Reactor Based on Surface Streamers for NO Conversion from N₂-O₂ Mixture Gases

M. A. Malik and K. H. Schoenbach

Frank Reidy Research Center for Bioelectrics, Old Dominion University, USA

Abstract—A novel pulsed corona discharge reactor is described which utilizes surface-plasma along insulating surfaces. The electrodes are comprised of a stainless steel wire anode of 150 μm diameter stretched along the surface of a glass sheet and two parallel aluminum strips as cathodes. An eight-stage Marx bank, which provides 60 ns, 40-45 kV monopolar pulses, was used to produce the surface streamers in nitrogen-oxygen mixtures at atmospheric pressure. With increasing oxygen content, the energy efficiency for NO₂ and O₃ synthesis was found to increase. The energy efficiency is almost the same for the surface-plasma and volume-plasma. However, the surface-plasma was found to be significantly more energy efficient than the volume-plasma for conversion of dilute NO in a feed gas containing 0-15% oxygen and with the balance being nitrogen. It is explained on the basis of surface-mediated reactions, the electric wind effect, and the diffusivity of the plasma which covers a larger fraction of the volume of the discharge gap as compared to volume-plasma. The surface-plasma reactor will be used to explore the treatment of NO_x and hydrocarbons in diesel engine exhaust.

Keywords—NO_x conversion, ozone synthesis, nitrogen fixation, non-equilibrium plasma, surface flashover

I. INTRODUCTION

Streamers along insulating surfaces have been studied mainly for the purpose of determining the dielectric strength of insulators in high voltage systems [1, 2]. Modeling results show that the surface streamers consist of a positive streamer head followed by quasi-neutral plasma in the channel behind the head and surrounded by a layer of positive charges [3]. This model explains the measured positive residual charge on the surface. Experimental results also indicate that the insulating surface plays a major role in the development of the surface-plasma. For example, photo-electron emission from the surface is believed to increase the ionization rate, which explains the faster speeds of surface streamers as compared to streamers in the gas alone [1, 2].

Interest in the application of surface-plasmas for environmental pollution control is growing because of their better energy efficiency as compared to the corresponding volume-plasmas [4-7]. For example, conversion of NO [4], destruction of toxic VOCs [5] and synthesis of O₃ [6] from air have been compared in surface-plasma and volume-plasma in a dielectric barrier discharge reactor all showing better energy efficiency with surface-plasma as compared to volume-plasma. A significant improvement in energy efficiency for destruction of toxic VOCs in a surface-plasma as compared to the volume-plasma in a pulsed corona discharge reactor has been reported [7]. Conversion of NO from N₂ + O₂ mixtures in the surface-plasma and the corresponding volume-plasma in a pulsed corona discharge reactor is being reported in this manuscript.

II. EXPERIMENTAL

The experimental setup employed in this study is shown in Fig. 1. The pulsed power system comprises a DC high voltage power supply and an 8-stage Marx bank. The total capacitance (C) of the Marx bank after switching is 0.29 nF, and the inductance (L) of the circuit is 1.53 μH . In order to obtain monopolar pulses, the resistive load (R) must exceed $2(L/C)^{1/2}$. The shortest possible monopolar pulse duration for an LCR circuit is obtained when $R = 2(L/C)^{1/2}$ (critically damped pulse). For the Marx circuit, the resistance has been calculated as $R = 146 \Omega$. This is a value that is small compared to the resistance of the streamer discharge. Therefore, placing two resistors of 75 Ω each in parallel to the discharge guarantees that the voltage pulse applied to the discharge is always the same, even when the discharge resistance fluctuates.

Voltage and current waveforms were recorded on an oscilloscope (Tektronix TDS 3052). The voltage probe was a Tektronix P6015A with a bandwidth of 75 MHz. Two 75 Ω resistors in series, both parallel to the load, were utilized as a 1:1 voltage divider. The current probe was a Pearson Electronics Current Monitor with a sensitivity of 0.1 V/A, and bandwidth of 20 MHz (Model 110A). The temporal resolution of the voltage and current traces is dependent on the bandwidth of the lowest bandwidth element in the diagnostic circuit, which in our case was the Pearson current probe. For consistency we have chosen a bandwidth of 20 MHz, by using a 20 MHz filter in the oscilloscope.

The electrical power was calculated as the product (VI) of the measured pulse voltage (V) and current (I). The energy per pulse (E_p) is the time integral ($\int VI dt$) of the power for the duration of the pulse. For each experiment, E_p was calculated from an average of 64 pulses and pulse frequency (f) from an average of 40

Corresponding author: Muhammad Arif Malik
e-mail address: mmalik@odu.edu

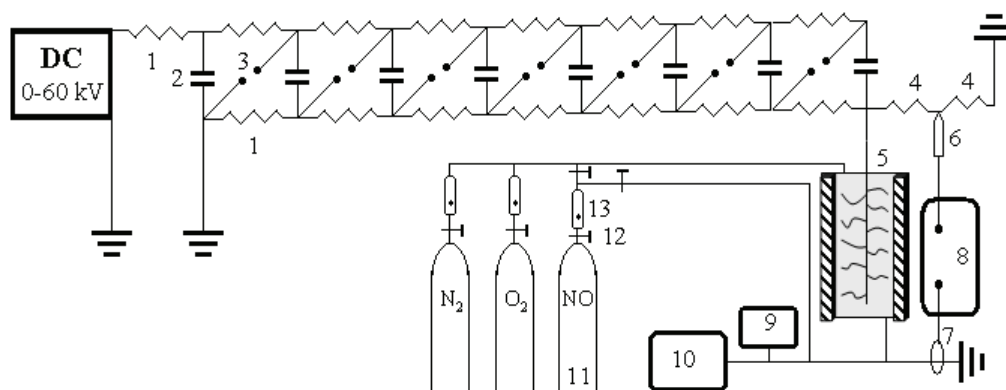


Fig. 1. Experimental setup: DC high voltage power supply connected to an 8-stage Marx bank and reactor. 1 = 100 k Ω resistors, 2 = 2.3 nF capacitors, 3 = spark gaps, 4 = 75 Ω resistors, 5 = reactor, 6 = high voltage probe, 7 = current probe, 8 = oscilloscope, 9 = NO_x analyzer, 10 = gas chromatograph, 11 = gas bottles, 12 = needle valves, and 13 = flow meters.

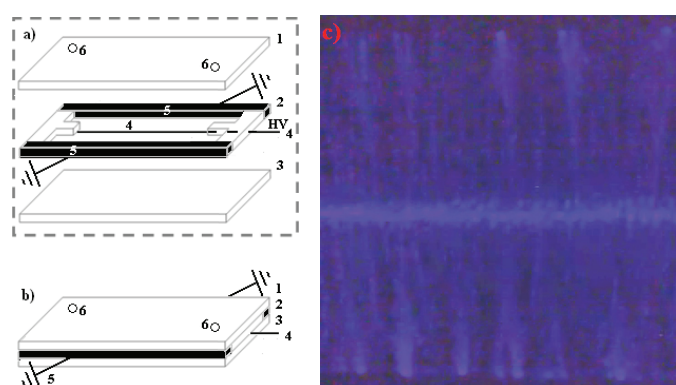


Fig. 2. Surface-plasma reactor: a) is a partially expanded view, and b) is view of the assembled reactor, and c) shows a time integrated image of the surface-plasma in nitrogen generated by a single voltage pulse. The components are: 1 and 3 are top and bottom glass sheets; 4 is the stainless steel wire anode of 150 μ m diameter; 2 is a spacer comprising Plexiglas or Teflon end fittings and cathodes (number 5) of aluminum forming two sides of the spacer, and 6 are gas inlet/outlet. The whole assembly is enclosed in two Plexiglas sheets held together by nuts and bolts and sealed by silicon sealant.

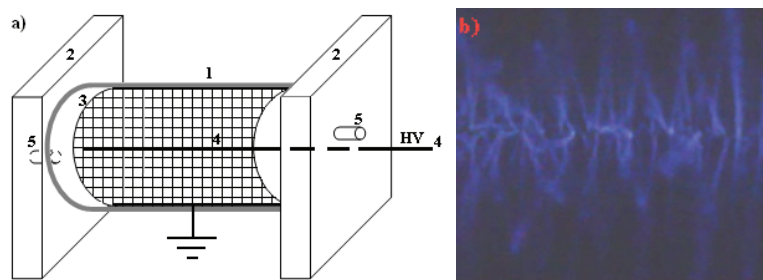


Fig. 3. Volume-plasma reactor : a) is a sketch of the reactor where the components are: 1 is a Plexiglas cylinder of 4.5 cm ID, 5.1 cm OD, and 15 cm length; 2 are Plexiglas end-fittings; 3 is a cylindrical cathode of 4.5 cm OD, 10 cm length, made of stainless steel mesh; 4 is a wire anode made of stainless steel wire of 150 μ m diameter and stretched along the axis of the cylinder; and 5 are gas inlet/outlet; b) shows a time integrated image of volume-plasma generated in nitrogen by a single voltage pulse.

pulses. The pulse frequency (f) was ~ 10 Hz in all experiments.

Fig. 2 shows the schematics of the surface-plasma reactor and a time-integrated image of the surface-plasma. The reactor comprises a wire to two parallel-plate electrodes stretched on the surface of a dielectric sheet and enclosed by another dielectric sheet with a spacer in between. The electrode lengths, inter-electrode gaps and thickness of the spacer that defines the volume of the discharge gap are listed in the results and discussion section. Fig. 3 shows the schematics of the volume-

plasma reactor in a wire-to-cylinder arrangement of electrodes and a time-integrated image of the volume-plasma.

Gases, i.e., N₂, O₂ and NO were supplied from high pressure gas bottles. Flow rates of the gases were controlled by needle valves and monitored with ball-float flow meters. A mixture of N₂ and O₂ with or without NO was passed through the reactor at a rate of 1 liter per minute (L/min) at a temperature of 25°C and one atmosphere of pressure in all experiments. The initial concentration of NO was 300 ppm in surface-plasma and

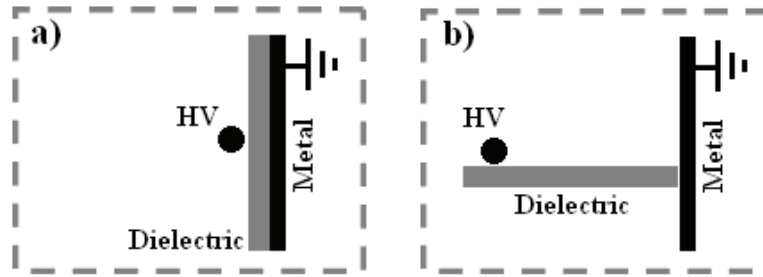


Fig. 4. Schematics of two commonly employed geometries of electrodes and dielectric surfaces for studies of surface plasma.

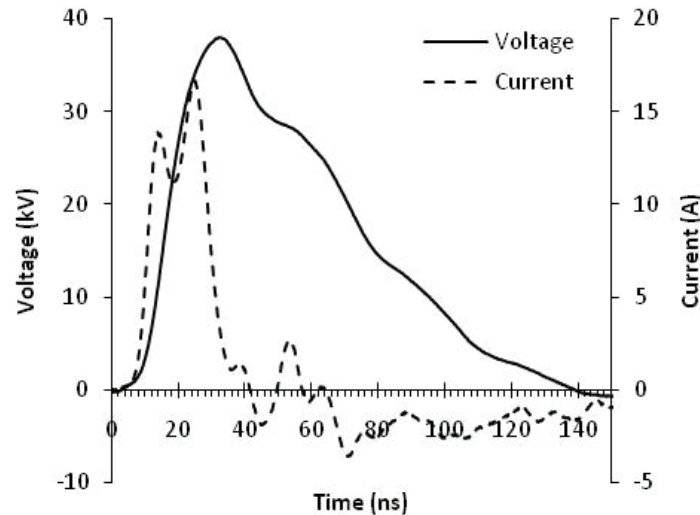


Fig. 5. Typical voltage and current waveforms in the surface-plasma reactor.

700 ppm in volume-plasma in all experiments, except where mentioned otherwise. The concentrations of O_2 , NO , and NO_2 were monitored by a NO_x analyzer (ENERAC Model 500, equipped with O_2 , NO and NO_2 sensors). Time-integrated images of single plasma discharges were recorded using a 5 mega-pixel camera.

III. RESULTS AND DISCUSSION

Fig. 4 illustrates two geometries of electrodes and dielectric surfaces usually employed for the study of surface-plasmas [2]. The geometry illustrated in Fig. 4a is similar to the geometry utilized in dielectric barrier discharges and the one illustrated in Fig. 4b is similar to that used for corona discharges, such as pulsed corona discharges. The latter is employed in the present study.

Two plasma reactors, i.e., a surface-plasma reactor (Fig. 2) and a volume-plasma reactor (Fig. 3) are employed in this study. The placement of electrodes on the dielectric surface ensured maximized surface-plasma formation in the surface-plasma reactor. In the case of the volume-plasma reactor, the cylinder electrode was kept 2.5 cm away from the end-fittings, which minimized the probability for the generation of surface-plasma due to the increased distance between the electrodes along the end-fitting surfaces. Therefore the reactor shown in Fig. 3 is optimized for volume-plasma.

Comparison of time integrated images of the plasmas show that the surface-plasma channels shown in Fig. 2c are thicker, more diffuse, and cover a larger fraction of the discharge gap compared with the volume-plasma channels shown in Fig. 3b, under the same experimental conditions.

The dielectric surface is likely to be charged positively [3] by the ions in the streamer. The resulting positive space charge causes a repulsive force on the positive surface charges surrounding the streamer. Since the expansion of the streamer towards the opposite dielectric surface is restricted to its positive surface space charge, the repulsive forces may lead to an expansion perpendicular to the streamer axis in the space between dielectric sheets rather than a shift away from the dielectric surface, and consequently, to a more diffuse streamer. This qualitative explanation would need to be confirmed by modeling.

Typical voltage and current waveforms observed in surface-plasma reactor are illustrated in Fig. 5. In the range of our experiments, changes in the ratio of oxygen and nitrogen concentrations did not seem to influence the pulse shapes significantly. The peak voltage was 40-45 kV, pulse rise time was ~ 15 ns, and pulse width at half maximum was ~ 60 ns.

The current reached a maximum value of ~ 16 A at ~ 25 ns and at a voltage of ~ 35 kV, still in the rising part of the voltage pulse. Visual observation and images of the discharge confirmed bridging of the electrode gap by

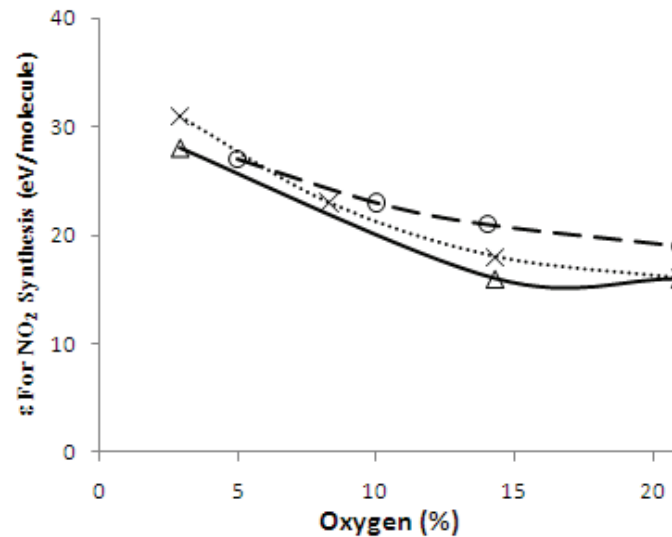
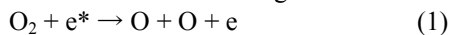


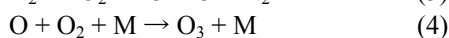
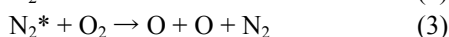
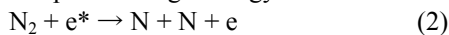
Fig. 6. Energy cost (ϵ) for NO_2 production versus oxygen concentration in the feed gas under three different conditions: ---○--- volume-plasma reactor,x..... surface plasma with spacer thickness 1.4 cm, and —△— surface plasma with spacer thickness 0.2 cm (the electrode lengths were 30 cm and the gaps between anode and cathode were 4.5 cm in both the surface plasma reactors).

surface streamers. We believe that a streamer-to-glow transition takes place after the streamers bridge the gap between the electrodes. The measured resistance at the peak current is $\sim 2 \text{ k}\Omega$, far above values for arcs. However, the point of transition from streamer to glow discharge could not be determined from the temporal development of voltage and current waveforms.

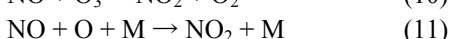
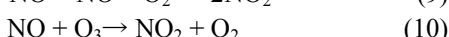
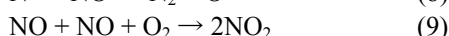
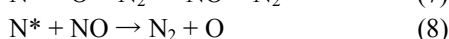
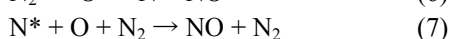
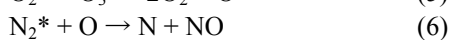
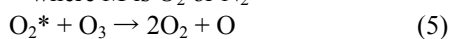
The electrical energy is mainly used for electron heating rather than gas heating in the plasma generated by high voltage pulses of sharp rise time and short duration [8]. High-energy electrons generated in the plasma collide with ambient gas molecules and dissociate them into free radicals, like O and N [9]. The radicals then react with each other and with ambient gas molecules and produce new compounds like NO, NO_2 , O_3 , etc., by reactions such as the following:



where * represents high-energy state.



where M is O_2 or N_2



The concentration of NO_2 in the treated gas indicates the amount of nitrogen- as well as oxygen-based active species produced in the plasma. NO_2 was measured in parts per million (ppm), volume-to-volume, in exhaust gas at 25°C and one atmospheric pressure after three minutes of plasma operation at 10 Hz. The energy cost (ϵ) in units of electron-volts per molecule (eV/molecule) was calculated using the formula: $\epsilon = 250$

$E_p f / (F \Delta \text{NO}_2)$, where F is the flow rate in liters per seconds (L/s) and ΔNO_2 is the change in concentration of NO_2 in ppm [10]. The energy yield (Y) in units of gram per kilowatt-hours (g/kWh) is calculated by using the formula: $Y = 37.3 M / \epsilon$, where M is molecular weight of the compound. It should be mentioned here that “energy efficiency” in this manuscript refers to energy yield (Y) and it is reciprocal of energy cost (ϵ).

Fig. 6 shows the energy cost for NO_2 production as a function of oxygen concentration in ambient gas in the volume-plasma reactor and two surface-plasma reactors: one having spacer thickness 1.4 cm, and the other 0.2 cm. The energy cost gradually decreased from $\sim 30 \text{ eV/NO}_2$ molecule (48 g/kWh) at 3% oxygen to $\sim 15 \text{ eV/NO}_2$ molecule (96 g/kWh) in air (20.9% oxygen) in all three reactors, in agreement with earlier studies [11]. The energy efficiency in volume-plasma and the surface-plasma reactors measured in this study is almost the same.

There was no NO detected in the exhaust gas. Ozone formed in the plasma reactor converts NO to NO_2 by reaction No. 10 [12], which explains the absence of NO in the treated gas. Ozone reacts preferentially with NO, but in the absence of NO it can oxidize NO_2 to higher oxidation states, such as NO_3 and N_2O_5 [12]. The oxides of nitrogen other than NO and NO_2 were not analyzed in this study.

In the present study, excess NO was mixed with the plasma exhaust and the reduction in the amount of NO was monitored. Energy cost for ozone in the plasma exhaust was calculated by assuming one molecule of ozone oxidized one molecule of NO to NO_2 . Fig. 7 shows that the energy cost for ozone production gradually decreased with an increase in oxygen content from $\sim 45 \text{ eV/molecule}$ ($\sim 34 \text{ g/kWh}$) at 3% oxygen to $\sim 13 \text{ eV/molecule}$ ($\sim 116 \text{ g/kWh}$) at 20.9% oxygen. Otherwise, the energy cost for ozone production was similar in the three reactors tested in this study.

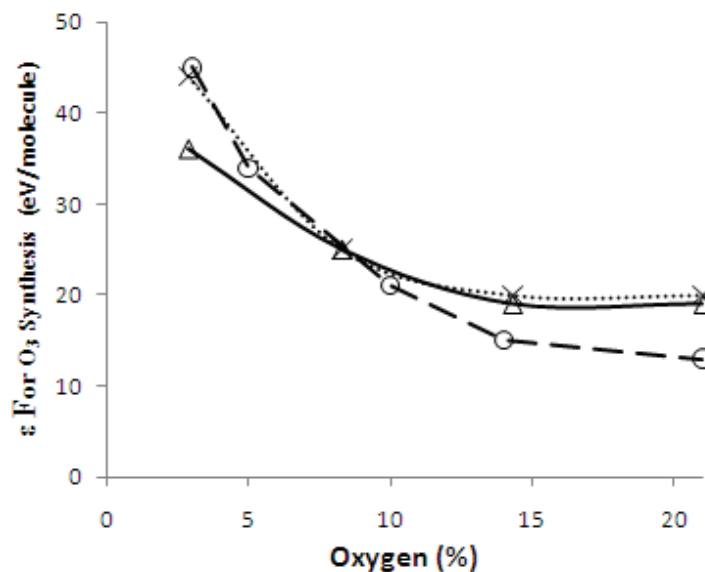


Fig. 7. Energy cost (ϵ) for O_3 production versus oxygen concentration in the feed gas under three different conditions: --○-- volume-plasma reactor,x..... surface plasma with spacer thickness 1.4 cm, and —△— surface plasma with spacer thickness 0.2 cm (the electrode lengths were 30 cm and the gaps between anode and cathode were 4.5 cm in both the surface plasma reactors).

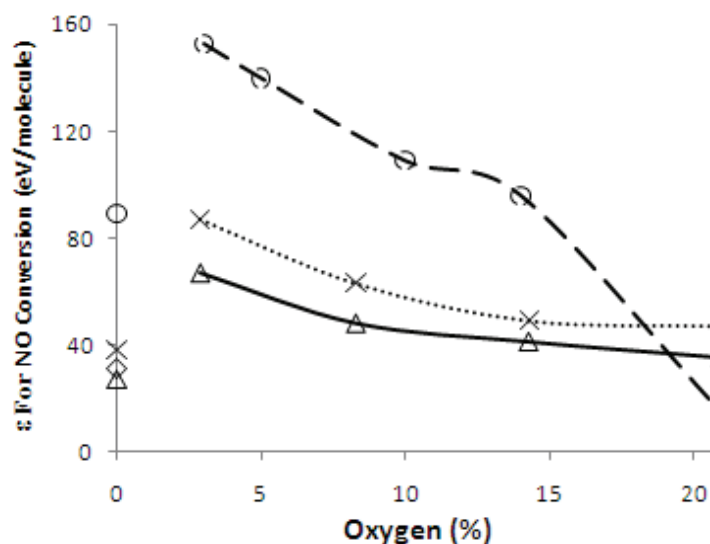


Fig. 8. Energy cost (ϵ) for NO conversion versus oxygen concentration in feed gas under three different conditions: --○-- volume-plasma reactor,x..... surface plasma with spacer thickness 1.4 cm, and —△— surface plasma with spacer thickness 0.2 cm (the electrode lengths were 30 cm and the gaps between anode and cathode were 4.5 cm in both the surface plasma reactors).

A major fraction of NO_x in flue gas is NO. The NO is relatively difficult to remove from the flue gas compared to higher oxidation states of nitrogen, such as NO_2 . The NO_2 is easier to remove, e.g., by scrubbing and chemical treatment [13]. This technique may be successful for NO_x treatment from stationary sources, such as coal or gas fired power plants. However, it is less likely to be applied in the case of mobile sources, such as diesel engine exhausts in vehicles, due to space limitations. Direct treatment by plasmas followed by hydrocarbon selective catalytic reduction (H-SCR) is being developed for treating NO_x from the diesel engine exhausts [14, 15]. In the direct treatment, the NO is oxidized to NO_2 and, at the same time, any unburned

hydrocarbons in the exhaust are activated by partial oxidation.

A synthetic mixture of $NO + N_2 + O_2$ was fed to the reactors for the direct plasma treatment. Fig. 8 shows the conversion of NO fed to the reactors. The production of NO_2 is not shown because when a synthetic mixture of NO and NO_2 (balance N_2) was analyzed, the accuracy of NO estimation was good (2% of the value), but accuracy of NO_2 was not. Further, NO_2 concentration exceeded the analyzable limits of 500 ppm in most of the experiments.

The energy cost for NO conversion was found to increase with a decrease in oxygen content from 20.9% to 3% and showed a sudden decrease in the case of pure nitrogen (0% oxygen) in the ambient gas in all the

reactors. These trends are in agreement with earlier studies [16].

The NO is removed either by reduction by N (reaction No. 8) or by oxidation by O or O₃ (reaction No. 10 & 11). The reduction by N is counterbalanced by NO formation (reaction No. 7). So, there is a net oxidation reaction responsible for NO removal [9]. The role of the oxidation reaction is further supported by the fact that the bond dissociation energy of O₂ (5.1 eV) is smaller than that of N₂ (9.8 eV). With a decrease in oxygen content in the ambient gas, oxidizing species like O and O₃ decrease. This explains the increase in energy cost for NO removal. In the extreme case of pure nitrogen, NO is removed by reduction with N, while the NO formation by N* becomes limited due to the absence of oxygen. It explains the low energy cost for NO removal in pure nitrogen as compared with the case of 3% oxygen mixed with nitrogen.

Fig. 8 shows that the surface-plasma is more energy efficient (lower energy cost) compared to the volume-plasma when oxygen in the ambient gas is less than that in air. Diesel exhaust contains oxygen in the range of 3–15%. The presence of unburned hydrocarbons in the case of real diesel engine exhaust will further increase the NO conversion significantly [9, 17]. These facts clearly indicate the advantage of using surface-plasma for treating diesel exhaust.

The energy cost for nitrogen-based and oxygen-based reactive species are expected to be almost equal for surface-plasma and volume-plasma, since the energy cost for their end products, i.e., NO₂ and O₃ are almost equal. So, the production of free radicals is less likely the factor responsible for the difference in the energy cost for NO conversions shown in Fig. 8. Nitrogen and oxygen molecules, being abundant in the treated gas, are available in sufficient concentration inside the plasma. So the reactive species do not need to enter the gas surrounding the plasma zone for production of NO₂ and ozone. NO, on the other hand, is in very low concentration and the reactive species formed in the plasma need to extend into the ambient gas. The diffuse nature of the plasma covering a larger fraction of the reaction zone in the case of surface streamers most probably extends the reach of the reactive species as compared with volume streamers.

Electric wind generated by the discharge is another factor considered responsible for efficient mixing and, consequently, energy efficient chemical conversion in surface dielectric barrier discharges [5]. Adsorption and stabilization of reactive species, such as, O [18] and N [19] from plasma onto glass and their availability for further oxidation reactions, such as oxidation of NO to NO₂ by reacting with adsorbed O [18] has been shown in recent literature. The surface-mediated reactions can also explain better energy efficiency in surface-plasmas compared to the volume-plasmas. The dielectric surfaces in the case of surface-plasma have a higher probability of adsorbing and stabilizing the reactive species due to their close proximity with the plasma compared to the case of volume-plasma. These three factors, i.e., diffused plasma,

electric wind, and surface mediated reactions, explain the lower energy cost for NO conversion in the surface-plasma than in the volume-plasma.

One exception to the general trend mentioned above is that the volume-plasma was more energy efficient for NO conversion from air (20.9% oxygen) than the surface-plasma. The reason for this reversal of the trend in air is not understood at this stage.

The energy per pulse was $\sim 100 \pm 10$ mJ in the case of volume-plasma and it was $\sim 35 \pm 8$ mJ in the case of surface-plasma employed for data shown in Figs. 6, 7 and 8. The energy cost for NO₂ and O₃ synthesis (Figs. 6 and 7) was almost the same, while the energy cost for NO conversion (Fig. 8) is slightly lower in surface-plasma in which the spacer thickness was 0.2 cm compared to the surface-plasma having space thickness of 1.4 cm. It means that the volume of the discharge gap of the surface-plasma reactor can be reduced from ~ 400 ml to ~ 50 ml by reducing the thickness of the spacer from 1.4 cm to 0.2 cm without reducing the energy efficiency.

Fig. 9 shows the dependency of energy cost on the degree of NO conversion in the volume-plasma and surface-plasma formed on Teflon or Plexiglas or glass dielectric. Energy per pulse was $\sim 100 \pm 10$ mJ in volume-plasma and $\sim 10 \pm 2$ mJ in surface-plasma employed for NO conversion shown in Fig. 9. In these experiments, the inlet concentration of NO was varied, which resulted in different degrees of NO conversions, keeping all other parameters the same. The energy cost increases with the degree of NO conversion. This is a general trend in any plasma treatment. The energy cost for surface plasma on glass, poly(methyl methacrylate) and teflon as dielectric layer is significantly lower compared to the volume plasma. For example, the energy cost at 50% NO conversion is 175 eV/molecule (6 g/kWh) in the case of volume plasma and is reduced in surface plasma to 97 eV/molecule (12 g/kWh) on Teflon, 74 eV/molecule (15 g/kWh) on poly(methyl methacrylate), and 51 eV/molecule (22 g/kWh) on glass.

Fig. 9 shows the order of energy cost with respect to the dielectric surface: Teflon > poly(methyl methacrylate) > glass. This trend indicates that the surface plasma strongly interacts with the dielectric surface. This is supported by the fact that the physical characteristics of the plasma are also dependent on the dielectric [1, 2]. Adsorption and stabilization of plasma-produced reactive species on quartz surfaces and their utilization in surface mediated chemical reactions has been reported [18, 19]. The glass surface employed in this study is closer to that of quartz and, consequently, more efficient for the surface mediated reactions, as compared to organic polymers like Teflon or poly(methyl methacrylate). The role of other factors, such as inter-electrode gap, effective length of the electrodes, applied voltage, pulse frequency and other dielectrics, especially porous ceramics having larger surface area, needs to be evaluated.

The energy efficiency for 50% NO conversion from nitrogen by volume-plasma reactor in this study (~ 6

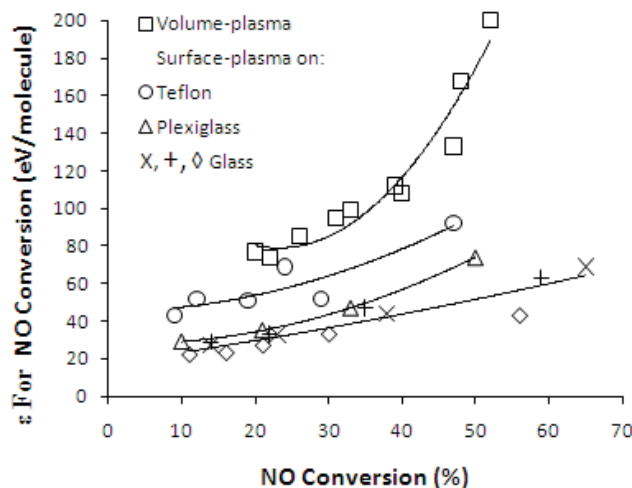


Fig. 9. Energy cost (ϵ) versus NO conversion (NO balance N_2). The points (\square , \circ , Δ , \times , $+$, & \diamond) represent experimental values and curves serve as a visual guide of the trends. The electrode lengths were 16.5 cm, the gaps between anode and cathode were 3.8 cm, and thickness of the spacer was 0.2 cm in the surface plasma reactors).

g/kWh) is the same as calculated from the data shown in earlier studies on pulsed corona discharges and dielectric barrier discharges [20]. It is comparable with ~ 5 g/kWh to that of semi-wet type pulsed corona discharges [21]. The energy efficiency was increased to about 22 g/kWh by employing surface-plasma in the present study. It should be mentioned that the pulsed corona discharge reactor employed in this study is not the optimum system for this application. Its energy efficiency can be improved further by additives and by varying electrical parameters. For example, additives, such as hydrocarbons [17] or ammonia [22] can significantly improve the energy efficiency for NO conversion in plasma reactors. Energy efficiency value of 125 g/kWh has been reported in a plasma reactor with ammonia addition [22]. A good example of energy efficiency improvement by varying electrical parameters is ~ 18 g/kWh energy efficiency for 50% NO conversion in a pulsed corona discharge reactor biased by very short 5 ns duration pulses [23]. The best energy efficiency in the present study was ~ 22 g/kWh achieved by employing the surface-plasma reactor.

IV. CONCLUDING REMARKS

1. Surface streamers generate a more diffuse plasma (filling a larger volume) than volume streamers.
2. Energy costs for production of ozone or NO_2 that require reactions with bulk gas molecules are nearly the same in surface streamer discharges as in volume streamer discharges.
3. Conversion of dilute pollutants like NO that require the extended reach of the reactive species into the ambient gas is more efficient in surface streamer discharges than in volume streamer discharges.
4. The width of the discharge space between the dielectric sheets can be reduced from 1.5 cm to 0.2

cm without reducing the energy efficiency for NO conversion.

5. The energy cost for the plasma chemical reactions, such as NO conversion, is dependent on the dielectric surfaces in the case of surface plasma.

ACKNOWLEDGMENT

This work is supported by the "Frank Reidy Fellowship in Environmental Plasma Research." The authors thank J. Thomas Camp for providing the Marx Bank and for helpful discussions related to the high voltage system. The authors thank Shu Xiao and Juergen F. Kolb for useful technical discussions. The authors thank Mr. Kevin Sullivan from ENERAC Inc. for re-checking cross-sensitivity of NO and NO_2 sensors when a mixture of NO and NO_2 (balance N_2) is fed to the NO_x analyzer employed in this study.

REFERENCES

- [1] N. L. Allen and P. N. Mikropoulos, "Streamer propagation along insulating surfaces," *IEEE Transactions on Dielectrics and Electrical Insulation*, vol. 6, pp. 357-362, 1999.
- [2] V. Bloschitsyn, "Review of surface discharge experiments," arXiv:1005.5044v1 [physics.plasm-ph], 2010.
- [3] A. Kumada, S. Okabe, and K. Hidaka, "Residual charge distribution of positive surface streamer," *Journal of Physics D: Applied Physics*, vol. 42, 095209, 2009.
- [4] E. Odic, M. Dhainaut, M. Petit, C. Karimi, A. Goldman, and M. Goldman, "Towards a better understanding of the electrical parameters monitoring the chemical reactivity of dielectric barrier discharges at atmospheric pressure," in *Proc. 3rd Int. Symp. Non-Thermal Technol. For Pollution Control, ISNTPT-3*, Seogwipo, Korea, pp. 62-67, 2001.
- [5] L. Oukacine, J. M. Tatibouet, J. Jolibois, and E. Moreau, "Ionic Wind Effect on the Chemical Reactivity," presented at International Symposium on Non-Thermal/Thermal Plasma Pollution Control Technology & Sustainable Energy, ISNTPT-7 June 21-25, 2010, St. John's, Newfoundland, Canada.

- [6] E. Odic, M. Dhainaut, M. Petit, A. Goldman, M. Goldman, and C. Karimi, "Approach of the Physical and Chemical Specific Properties of Pulsed Surface Dielectric Barrier Discharges in Air at Atmospheric Pressure," *Journal of Advanced Oxidation Technologies*, vol. 6, pp. 41-47, 2003.
- [7] M. A. Malik, Y. Minamitani, and K. H. Schoenbach, "Comparison of catalytic activity of aluminum oxide and silica gel for decomposition of volatile organic compounds (VOCs) in a plasmacatalytic Reactor," *IEEE Transactions on Plasma Science*, vol. 33, pp. 50-56, 2005.
- [8] S. Masuda, "Pulse corona induced plasma chemical process: a horizon of new plasma chemical technologies," *Pure and Applied Chemistry*, vol. 60, pp. 727-731, 1988.
- [9] B. M. Penetrante, R. M. Brusasco, B. T. Merritt, and G. E. Vogtlin, "Environmental applications of low-temperature plasmas," *Pure and Applied Chemistry*, vol. 71, pp. 1829-1835, 1999.
- [10] M. Gundersen, V. Puchkarev, A. Kharlov, G. Roth, J. Yampolsky, and D. Erwin, "Transient plasma-assisted diesel exhaust remediation," in *Low Temperature Plasmas. Fundamentals, Technologies, and Techniques* (2nd Edn.), Hippler R, Kersten H, Schmidt M, Schoenbach KH (Eds.), Wiley-VCH Verlag GmbH, Weinheim, pp. 543-550, 2008.
- [11] T. Namihira, S. Tsukamoto, D. Wang, S. Katsuki, R. Hackam, K. Okamoto, and H. Akiyama, "Production of nitric monoxide using pulsed discharges for a medical application," *IEEE Transactions on Plasma Science*, vol. 28, pp. 109-114, 2000.
- [12] Y. S. Mok, "Oxidation of NO to NO₂ using the ozonization method for the improvement of selective catalytic reduction," *Journal of Chemical Engineering of Japan*, vol. 37, pp. 1337-1344, 2004.
- [13] T. Kuroki, H. Fujishima, K. Otsuka, T. Ito, M. Okubo, T. Yamamoto, and K. Yoshida, "Continuous operation of commercial-scale plasma-chemical aftertreatment system of smoke tube boiler emission with oxidation reduction potential and pH control," *Thin Solid Films*, vol. 516, pp. 6704-6709, 2008.
- [14] B. M. Penetrante, R. M. Brusasco, B. T., Merritt, W. J. Pitz, G. E. Vogtlin, M. C. Kung, H. H. Kung, C. Z. Wan, and K. E. Voss, "Plasma-assisted catalytic reduction of NO_x," *SAE Technical Papers Series*, No. 982508, 1998.
- [15] Y. Itoh, M. Ueda, H. Shinjoh, K. Nakakita, and M. Arakawa, "NO_x Reduction under oxidizing conditions by plasma-assisted catalysis," *R&D Review of Toyota CRDL*, vol. 41, pp. 49-62, 2006.
- [16] Y. S. Mok, J. H. Kim, I. S. Nam, and S. W. Ham, "Removal of NO and formation of byproducts in a positive-pulsed corona discharge reactor," *Industrial and Engineering Chemistry Research*, vol. 39, pp. 3938-3944, 2000.
- [17] Y. S. Mok and I. S. Nam, "Role of organic chemical additives in pulsed corona discharge process for conversion of NO," *Journal of Chemical Engineering of Japan*, vol. 31, pp. 391-397, 1998.
- [18] O. Guaitella, M. Hübner, S. Welzel, D. Marinov, J. Röpkke, and A. Rousseau, "Evidence for surface oxidation on Pyrex of NO into NO₂ by adsorbed O atoms," *Plasma Sources Science and Technology*, vol. 19, 045026 (5 pp.), 2010.
- [19] D. Marinov, O. Guaitella, A. Rousseau, and Y. Ionikh, "Production of molecules on a surface under plasma exposure: Example of NO on pyrex," *Journal of Physics D: Applied Physics*, vol. 43, 115203, 2010.
- [20] B. M. Penetrante, M. C. Hsiao, B. T. Merritt, G. E. Vogtlin, P. H. Wallman, M. Neiger, O. Wolf, T. Hammer, and S. Broer, "Pulsed corona and dielectric-barrier discharge processing of NO in N₂," *Applied Physics Letters*, vol. 68, pp. 3719-3721, 1996.
- [21] A. Mizuno, A. Chakrabarti, and K. Okazaki, "Application of corona technology in the reduction of greenhouse gases and other gaseous pollutants," in *NATO ASI Series, Vol. G 34, Part B, Non-thermal plasma techniques for pollution control*, B. M. Penetrante, S.E. Schultheis, Eds, Springer-Verlag, Berlin Heidelberg, pp 165-185, 1993
- [22] J. S. Chang, K. Urashima, Y. X. Tong, W. P. Liu, H. Y. Wei, F. M. Yang, and X. J. Liu, "Simultaneous removal of NO_x and SO₂ from coal boiler flue gases by DC corona discharge ammonia radical shower systems: Pilot plant tests," *Journal of Electrostatics*, vol. 57, pp. 313-323, 2003.
- [23] T. Matsumoto, D. Wang, T. Namihira, and H. Akiyama, "Energy Efficiency Improvement of Nitric Oxide Treatment Using Nanosecond Pulsed Discharge," *IEEE Transactions on Plasma Science*, vol. 38, pp. 2639-2643, 2010.